

## TRANSVERSAL RESISTANCE OF LONG-FIBRE COMPOSITES: INFLUENCE OF THE FIBRE-MATRIX INTERFACE

V. Carvelli, A. Corigliano

Department of Structural Engineering, Technical University (Politecnico) of Milan,  
Piazza Leonardo Da Vinci 32 , Milan (Italy)

### ABSTRACT

In this work, the 2D finite element model presented in [1], and extended to 3D in [2], is used to predict the macroscopic mechanical properties of unidirectional fibre reinforced composites (FRC) taking into consideration the fibre-matrix interface behaviour. The numerical model is based on the homogenisation theory for periodic media. The finite element model of the Representative Volume provides the macroscopic mechanical behaviour taking into consideration two kinds of fibre-matrix interface: the first with perfect adhesion, the second with no resistance in tension, thus simulating a completely debonded interface.

**Keywords:** long-fibre composite, fibre-matrix interface, mechanical properties.

### INTRODUCTION

Fibre reinforced composites (FRC) are used in almost every type of advanced engineering structure, e.g. aircraft, boats, automobile, sports goods and civil infrastructures.

The usage of FRC continues to grow at an impressive rate. The key factors driving the increase in applications are mainly the continuous improvement of the manufacturing techniques and the development of analytical and numerical tools to design and predict their mechanical response [3].

In this work, the 2D finite element model presented in [1], and extended to 3D in [2], is used to predict the macroscopic mechanical properties of unidirectional fibre reinforced composites taking into consideration the fibre-matrix interface behaviour. The numerical model is based on the homogenisation theory for periodic media [4]. The overall, or macroscopic, properties of FRCs can be predicted by analysing a Representative Volume (RV) with suitable boundary conditions to enforce the periodicity of the material. The particular case of periodic hexagonal reinforcing array is considered and the relevant finite element model used to numerically predict the mechanical properties.

Two kinds of fibre-matrix interfaces have been considered: the first with perfect adhesion, the second with no resistance in tension, thus simulating a completely debonded interface. In order to avoid fibre-matrix inter-penetration, unilateral contact conditions have been used.

Uniaxial and biaxial tractions, in the plane orthogonal to the fibres direction, are simulated on a unidirectional FRC having different fibre volume fractions. The representative volume is composed of an elastic fibre inside an elastic-perfectly plastic matrix complying with von Mises failure domain. The numerical analyses are performed assuming a plane strain state.

The results of this academic applications shows the importance of the fibre-matrix interface behaviour on the global mechanical response of the composite materials. This preliminary

conclusion will be supported by comparisons with experimental results and other numerical predictions in forthcoming works.

## NUMERICAL HOMOGENIZATION METHOD

The numerical model for the analysis of the considered FRC is now summarized. The approach was proposed in [1] for two-dimensional analyses in the plane perpendicular to the fibres and extended to general macroscopic three-dimensional stress states in [2].

### Problem Formulation

The reinforcing array of the composite consists of equal parallel fibres of circular cross section (see Figure 1a), that are evenly arranged according to a regular hexagonal pattern. Thus, the problem can be studied within the framework of the micromechanical theory of heterogeneous, periodic materials [4].

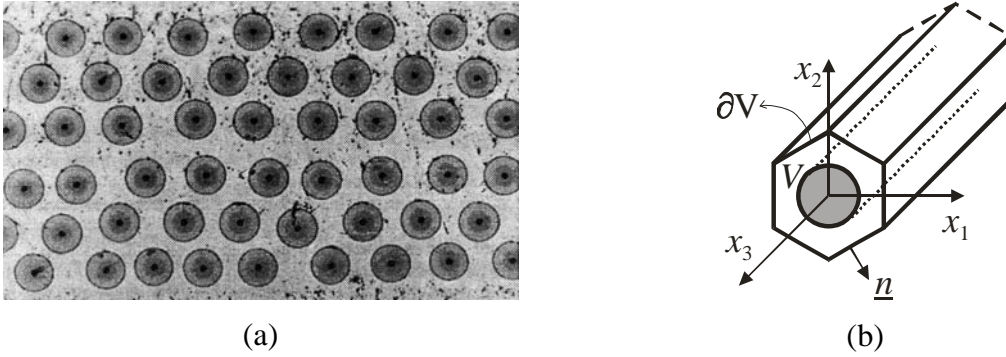


Figure 1. (a) Composite with long parallel unidirectional fibres; (b) Representative Volume (RV) for a regular hexagonal pattern.

The global response of the composite is determined through the analysis of any Representative Volume (RV). For the composites examined, a possible RV is shown in Figure 1b. Let  $V$  denote the volume of the RVE and let  $x_3$  denote the fibre axis, so that  $x_1, x_2$  are the orthogonal axes lying in any plane perpendicular to the fibres (see Figure 1b).

The macroscopic (global) constitutive law describes the relation between macroscopic stresses and strains tensors ( $\underline{\underline{\Sigma}}, \underline{\underline{E}}$ ), defined as volumetric averages of the relevant microscopic variables ( $\underline{\underline{\sigma}}(\underline{x}), \underline{\underline{\varepsilon}}(\underline{x})$ ) that are functions of the position vector  $\underline{x}$  in the representative volume (RV) (double-underlined and underlined symbols denote 2<sup>nd</sup> order tensors or matrices and vectors respectively).

For composites consisting of non-linear components, this law has to be determined in incremental form. The macroscopic constitutive law actually describes the global response of any RV belonging to an ideal infinite medium subjected to uniform boundary conditions, either in stresses or displacements. Accordingly, the local (microscopic) stress and strain fields are of suitable form.

Due to geometry and material invariance of the RVE along the fibre direction, the microscopic strain field does not depend on  $x_3$ :  $\underline{\underline{\varepsilon}} = \underline{\underline{\varepsilon}}(x_1, x_2)$ ; furthermore, in the plane  $(x_1, x_2)$ ,  $\underline{\underline{\varepsilon}}$  has to comply with the periodicity of the reinforcing array.

In order to fulfil a strain field with the characteristics outlined above, the following general 3D microscopic displacement field is assumed [1, 2]:

$$\underline{u}(x_1, x_2, x_3) = \underline{u}_0 + \underline{\underline{\Omega}} \cdot \underline{x} + \underline{\underline{E}} \cdot \underline{x} + \tilde{\underline{u}}(x_1, x_2) \quad (1)$$

where  $\underline{u}_0$  represents a rigid displacement of the RV and  $\underline{\Omega}$  is the anti-symmetric tensor related to the small rigid rotation of the RV. The pure strain modes of the RV are described by the last two terms in (1): a constant term (the macroscopic strain  $\underline{E}$ ) and a  $V$ -periodic term, with zero average value, associated with the  $V$ -periodic part  $\tilde{\underline{u}}$  of the microscopic displacement field.

The incremental problem that allows the definition of the macroscopic constitutive law can be expressed as follows:

$$\text{div } \underline{\underline{\dot{\sigma}}} = \underline{\underline{0}} \quad \text{in } V; \quad \underline{\underline{\dot{\sigma}}} = F(\underline{\underline{\dot{\epsilon}}}(\underline{\underline{\dot{u}}})) \quad \text{in } V \quad (2a,b)$$

$$\underline{\underline{\dot{u}}} = \underline{\underline{\dot{u}}} - \underline{\underline{\dot{E}}} \cdot \underline{\underline{\dot{x}}} \quad V - \text{periodic}; \quad \underline{\underline{\dot{t}}} = \underline{\underline{\dot{\sigma}}} \cdot \underline{\underline{n}} \quad \text{anti - periodic on } \partial V \quad (2c,d)$$

$$\underline{\underline{\dot{\Sigma}}} = \frac{1}{V} \int_V \underline{\underline{\dot{\sigma}}} dV; \quad \underline{\underline{\dot{E}}} = \frac{1}{V} \int_V \underline{\underline{\dot{\epsilon}}} dV \quad (2e,f)$$

where  $\partial V$  indicates the boundary of the RV;  $\underline{\underline{n}}$  is the outward unit-normal to  $\partial V$ . Eqn. (2a) is the microscopic equilibrium equation; eqn. (2b) represents the microscopic incremental constitutive law while eqn. (2c) and eqn. (2d) are the periodic kinematics and static boundary conditions respectively. The definition of the macroscopic quantities ( $\underline{\underline{\Sigma}}$ ,  $\underline{\underline{E}}$ ) is expressed by eqns. (2e,f).

### Finite element model

A model based on the finite element method in the displacement formulation has been used to solve the incremental problem (2).

The mesh used in the numerical analyses is shown in Figure 2. This 2D mesh is the same used in [1] for the analysis of a RVE subjected to stresses in a plane normal to the fibres. In [2] this mesh was modified in order to consider a three-dimensional macroscopic stress state.

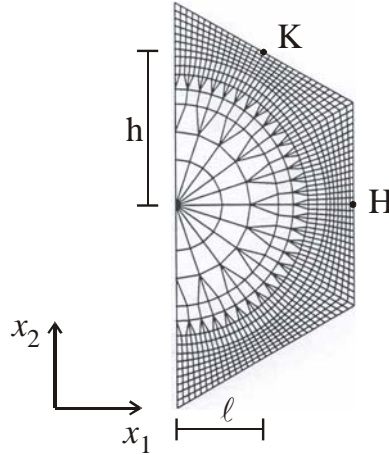


Figure 2. Finite element model of the RV.

The main task to implement problem (2) in a displacement-based FE code is the assignment of the boundary conditions to ensure that the displacement field complies with eqn. (1). Details on the boundary conditions applied to the hexagonal RV used are described in [1] for the 2D problem and in [2] for its 3D extension.

Here, the kinematic boundary conditions that allow for the simulation of any prescribed macroscopic strain state in a plane normal to the fibres, through only some free nodal displacements (e.g.  $u_{1,H}$ ,  $u_{2,H}$ ,  $u_{2,K}$ ), are only summarized. These conditions are:

$$E_{11} = u_{1,H} / \ell; \quad E_{22} = (u_{2,K} - u_{2,H} / 2) / h; \quad E_{12} = u_{2,H} / \ell \quad (3a,b,c)$$

where H and K represent the mid points of the model edges (see Figure 2);  $h$  and  $\ell$  describe the geometric properties of the RV (see Figure 2).

In the numerical simulations, macroscopic strain components are prescribed by (3) and the macroscopic stress tensor is evaluated by the volumetric average (2e) of the microscopic counterpart in the Gauss integration points.

## NUMERICAL RESULTS

The model presented in the previous section has been applied to the simulation of uni- and biaxial tests on unidirectional FRC having isotropic elastic fibres and an elastic-plastic matrix obeying the von Mises yield criterion (being  $\sigma_0$  the yield stress). The assumption of plane strain behaviour restricts our attention to the analysis of the material behaviour in the plane perpendicular to the fibres direction.

A commercial finite element code [5] was employed to obtain the numerical results listed in the following.

The finite element model of the RV takes into consideration the fibre-matrix interface. The difficulty in knowing *a priori*, in the material design phase, the mechanical features of the fibre-matrix interface has suggested to the Authors the choice of two kinds of interface behaviour: the first gives a perfect adhesion, the second simulates the absence of resistance in tension and shear, i.e. a completely debonded interface. In order to avoid fibre-matrix interpenetration, unilateral contact conditions have been imposed. These assumptions allow to obtain the bounds in which the mechanical properties of the real unidirectional FRP, with its fibre-matrix interface, should be contained.

The influence of the fibre-matrix interface on the elastic properties of the composite is first presented; subsequently, the consequences of different interface behaviours on the failure property of the composite is discussed.

The mechanical features of the components (polymeric matrix and glass fibres) employed in the numerical analyses are listed in Table 1.

	Elastic modulus: E [MPa]	Poisson's ratio: $\nu$	Yield stress: $\sigma_0$ [MPa]
Matrix	3280	0.31	99.5
Fibre	71600	0.22	--

Table 1. Mechanical features of the components.

The elastic modulus for traction in  $x_1$  direction (see Figure 2) of two RV having perfect and debonded interfaces is presented in Figure 3 (being  $E_0$  the matrix elastic modulus). Increasing the fibre volume fraction  $c_f$ , the elastic modulus of the composite with perfect interface increases more rapidly with respect to the case with debonded interface. On the contrary, for a uni-axial compression in  $x_1$  direction, increasing the fibre volume fraction  $c_f$ , the elastic modulus for a perfect and dedonded interface almost coincide (see Figure 4).

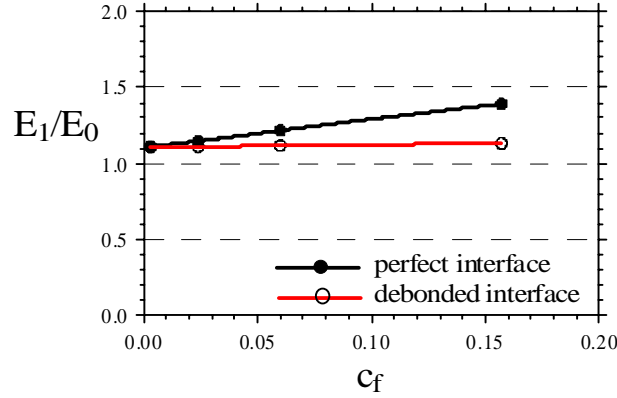


Figure 3. Elastic modulus for traction along  $x_1$  direction: comparison between the composite with perfect and debonded interface.

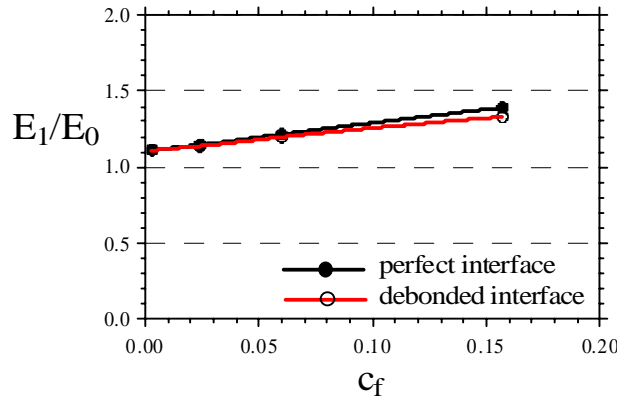


Figure 4. Elastic modulus for compression along  $x_1$  direction: comparison between the composite with perfect and debonded interface.

Figure 5 shows the macroscopic failure stress, for uni-axial tension along  $x_1$  (see Figure 2), as a function of the fibre volume fraction  $c_f$  (being  $\sigma_0$  the matrix yield stress). The comparison between the composites with perfect and debonded interface shows a drastic reduction of the strength for the fibre contents considered (small values with respect to the usual production). A different consideration can be done for the uni-axial compression strength along  $x_1$  (see Figure 6). In fact, increasing the fibre volume fraction  $c_f$  the strength in compression of the FRC with debonded interface has a reduction (the absolute value decreases) with respect to the perfect interface but the region contained in the two bounds is much more narrow in comparison to the case of tensile failure.

The deformed shape of the RV after a traction along  $x_2$  direction is depicted in Figure 7 for a fibre volume fraction  $c_f=0.157$ . The comparison between the complete debonded interface (Figure 7b) and the perfect interface (Figure 7a) shows the difference of the mechanism involved in the failure of the material subject to uni-axial tension. The failure mechanisms became evident in the observation of the equivalent plastic strain contour plots in Figure 8. The strain concentration highlights the regions in which the failure takes place. The perfect and debonded interfaces provide different strain concentration zones, i.e. different failure mechanisms.

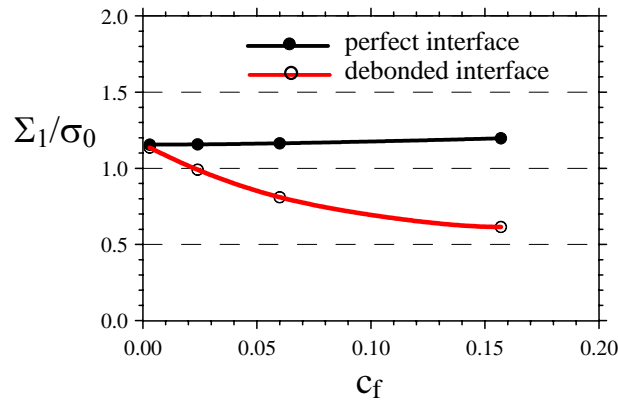


Figure 5. Strength for traction along  $x_1$  direction: comparison between the composite with perfect and debonded interface.

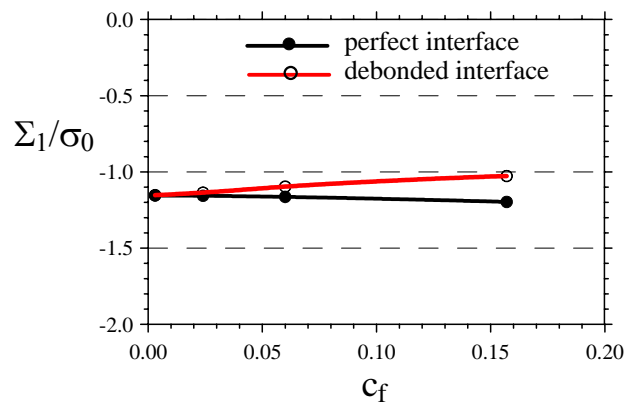


Figure 6. Strength for compression along  $x_1$  direction: comparison between the composite with perfect and debonded interface.

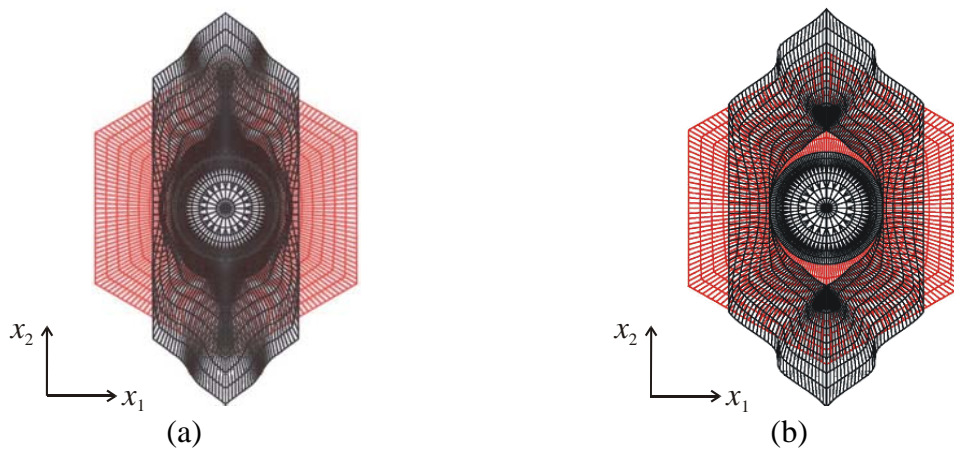


Figure 7. Deformed shape of the RV finite element mesh for a traction along  $x_2$  ( $c_f=0.157$ ): (a) perfect and (b) debonded interface.

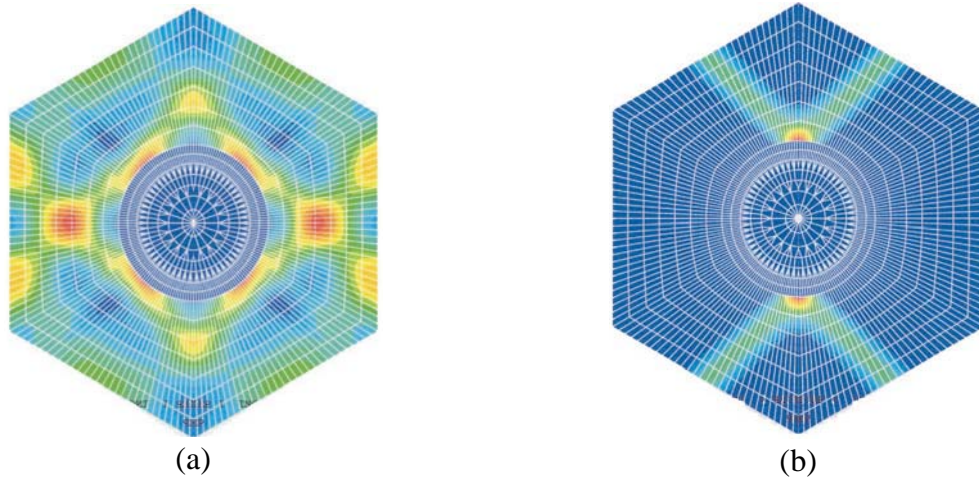


Figure 8. Contour plot of the equivalent plastic strain for a traction along  $x_2$  ( $c_f=0.157$ ):  
 (a) perfect and (b) debonded interface.

Having assumed an elastic-perfectly plastic matrix obeying the von Mises yield criterion, the failure domain in the macroscopic stress plane  $\Sigma_1$ - $\Sigma_2$  is represented, for a perfect fibre-matrix adhesion, by the two straight lines showing an infinite resistance for a bi-axial hydrostatic traction (see Figure 9). The failure domain for a complete debonded interface represented in Figure 9, for a RV with  $c_f=0.157$ , shows a finite resistance of the material subjects to a stress state along the hydrostatic axis. This remarkable difference in the failure domains for materials having the two extreme interface behaviours here considered, shows that the influence of the real FRC interface on the overall resistance should not be neglected. Moreover, the overall strength of the composite is lower than the strength of the matrix for a macroscopic stress state involving the components  $\Sigma_1$  and  $\Sigma_2$  (Figure 9), this means that the interface mechanical features are crucial in the prediction of the overall strength domain of the unidirectional FRC materials.

These considerations became more evident when the fibre volume fraction  $c_f$  increases. In Figure 10, the failure domains of materials with complete debonded interface are depicted for two different value of  $c_f$ . The larger is the fibre volume fraction, the smaller is the failure domain of the material (Figure 10). In fact, increasing the fibre volume fraction, the fibre-matrix interface surface increases and the influence of its mechanical features on the global strength of the material increases. Therefore, the knowledge of the interface properties are indispensable in particular for composite material with an high fibres content.

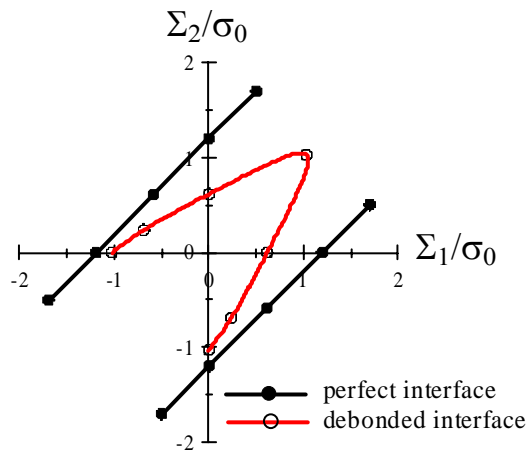


Figure 9. Strength domains of the composite with perfect and debonded interface ( $c_f=0.157$ ).

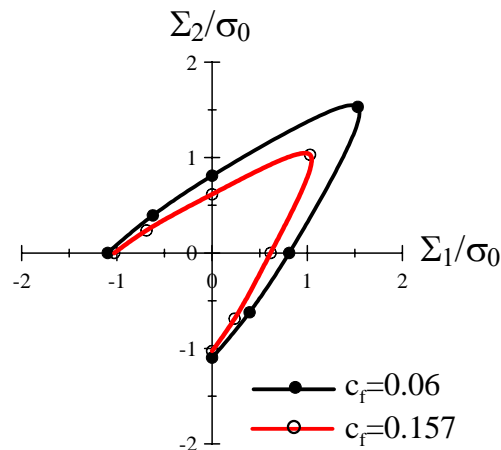


Figure 10. Comparison of strength domains for composites with debonded interface having different fibre volume fraction  $c_f$ .

## CONCLUSIONS

A comparative analysis of the elastic and strength properties of composites with perfect and debonded interfaces has been presented in this paper.

The methodology here applied, which is an extension of the previous works [1] and [2], has a general validity. The results here presented, in spite of being referred to low fibre volume fractions, clearly show the importance of considering the correct interface behaviour for the assessment of failure conditions in the plane orthogonal to the fibre direction.

In order to obtain further information on the influence of the fibre-matrix interface behaviour on the overall strength properties of the composites, the following issues should in particular be considered: introduction of more reliable interface models; experimental identification of interface properties; three dimensional simulations for the computation of three dimensional failure domains; experimental validation of the obtained results.

## REFERENCES

1. Taliercio A., Coruzzi R., "Mechanical behaviour of brittle matrix composites: a homogenization approach", *Int. Journal of Solids and Structures*, 36/24 (1999), 3591-3615.
2. Carvelli, V., Taliercio, A., "A Micromechanical model for the analysis of unidirectional elastoplastic composites subjected to 3D stresses", *Mechanics Research Communications*, 26/5 (1999), 547-553.
3. Herakovich, C. T., "Mechanics of fibrous composites", John Wiley & Sons, (1998).
4. Suquet, P., "Elements of homogenization for inelastic solid mechanics", In E. Sanchez-Palencia and A. Zaoui eds. 'Homogenization techniques for composite media', *Lecture Notes in Physics 272*, Springer, Wien, 193-278, (1985).
5. ABAQUS release 6.4, user's manual, (2003).